RESISTIVITY INDEX MEASUREMENTS UNDER WEAK CAPILLARY FORCES

By

Jos G. Maas, Niko van der Post, Krijn H. van der Gyp, John G.C. Coenen and Wim J. Looyestijn

Shell Technology Exploration and Production B.V.
Rijswijk
The Netherlands

Abstract

For log calibration, saturation exponents are determined in the laboratory through resistivity index measurements. Commonly, the well-known continuous injection (CI) technique is employed: oil is injected into a brine-saturated core. The standard measurement protocol calls for the resistivity to be measured across the sample and plotted versus the average brine saturation as determined by material balance.

This method hinges on the assumption that the saturation profile in the sample is flat, i.e. the local saturation at each point in the sample equals the average saturation. Since at the injection-end the oil saturation tends to be highest, one has to rely on the presence of a capillary pressure gradient that will flatten the saturation profile. By keeping the injection rate low, capillary forces may dominate viscous forces and achieve the required effect.

This contribution starts out to discuss simulations of experiments that show how certain rock may never produce the right data in a CI experiment. When a low capillary gradient occurs, a so-called Buckley-Leverett shock front travels through the sample during CI, and the I-Sw relationship has a distinct curvature on a log-log plot. A significant deviation from the true I-Sw relationship will result in an erroneous saturation log calibration.

Subsequently, we show how the Steady-State technique can be employed to overcome this measurement artefact. With this technique, water and oil are injected simultaneously and the development of a shock front is kept under control. The saturation distribution in the sample is measured through X-ray absorption. Resistivity is measured using electrodes along the sample.

By varying the ratio of the injected water and oil, different saturations can be achieved and a resistivity plot generated. Corrections due to the removal of the CI measurement artefact may amount to saturation shifts by 20 or more saturation units.

Introduction

For many years, the continuous injection (CI) method [1] has established itself as the laboratory measurement to calibrate resistivity logs. In essence, parameters are measured that characterise resistivity R as a function of the brine saturation S_w:

$$R(S_w) = R_0 S_w^{-n} \quad \text{Eq. 1}$$

with R_0 the resistivity of the sample at 100% brine saturation and n is Archie's saturation exponent. R_0 is dependent on sample porosity j and conductivity:

$$R_0 = R_w F \quad \text{Eq. 2}$$

with Rw the conductivity of the brine and F the formation factor:

$$F = a j^{-m} \quad \text{Eq. 3}$$

a is called the Humble factor and m the cementation index.

The measurement is conducted as follows. The cleaned sample is mounted in a Hassler-type core holder with a water-wet filter pushed against the outflow-end of the sample. The sample is saturated at 100% brine. This brings the sample to a condition thought to be representative of the virgin reservoir, before charging with hydrocarbons occurred. Oil is then injected into the plug to simulate that charging. During the injection, the resistivity of the sample is measured. The average brine saturation is determined simply from material balance. The water-wet filter prohibits production of hydrocarbons; therefore the injected oil or the produced brine is a direct measure for the average saturation change in the plug. A resistivity index plot is generated by plotting $I(S_w) = R(S_w)/R_0$ versus S_w on a log-log plot. The saturation exponent is extracted from the slope and used for resistivity log calibration.

Archie's formulation has been refined by several authors to account for clay conductivity [2] and other effects. The measurement method has been refined e.g. to address wettability problems by using aged core plugs and crude oil [3]. However, the basic measurement principle has remained the same: a primary drainage flooding experiment is conducted similar to an Unsteady-State or "Welge" experiment [4]. It is well known that Welge experiments exhibit a sizeable saturation shock-front that travels through the plug and that such a saturation discontinuity will interfere with a resistivity index measurement. As mentioned above, the average saturation is used in the log-log plot and therefore it is imperative that the saturation profile that exists in the plug during the drainage does not deviate much from the average saturation. A sharp and large shock front violates this assumption. Capillary forces, always present, tend to distort the shock front and to flatten-out the saturation profile. To allow the capillary forces to dominate the saturation profile, standard measurement procedures call for low injection rates (e.g. 1 PV per 2 weeks [5]).

This contribution addresses the fact that some plugs may have very small capillary pressure gradients over the range of the saturation shock and that the results obtained by normal injection rates may be wrong by 20 or more saturation units.
To that end, we will discuss in detail the CI technique and development of a saturation shock front. Subsequently, we will discuss how the flooding arrangement of the Steady-State (SS) technique, together with in-situ saturation monitoring can be used to obtain more representative resistivity index measurements. We have developed and tested such apparatus, of which the measurement results are presented in another SCA 2000 paper [6].

Displacement by Continuous Injection

The CI technique requires the injection of kerosene or another hydrocarbon into a plug saturated initially at 100% brine (Fig. 1). A water-wet filter is mounted to greatly facilitate the measurement of the average brine saturation by material balance, during the displacement. The displacement characteristics depend on the fractional flow function f_w [7].

Zero capillary pressure
In the absence of capillary pressure and gravity we have for f_w at any point in the plug:

$$f_w = \frac{q_w}{q_w + q_o} = \frac{1}{1 + \dfrac{k_{ro}/m_o}{k_{rw}/m_w}} = \frac{1}{1 + \dfrac{m_w}{m_o}\dfrac{k_{ro}}{k_{rw}}} \qquad \text{Eq. 4}$$

For an explanation of symbols, please see the nomenclature. We note that f_w is a function of the viscosity ratio and of the water saturation. A typical f_w plot is shown in Fig. 2. A shock front will develop with saturation S_f. As first shown by Welge [8], S_f can be found by drawing a straight line from the starting position of the drive, and tangent to the f_w function (see Fig.2). Note that for resistivity measurements by CI, we are in drainage mode and S_{wi}=1.

At constant injection rate, the shock front saturation travels at constant speed [7]

$$v_f = \frac{q_t}{Aj}\left(\frac{df_w}{dS_w}\right)_{S=S_f} \qquad \text{Eq. 5}$$

Upstream of the front, a saturation profile develops according to the formulation first developed by Buckley and Leverett [9] (B-L). These authors also described the shock front, but in a less accessible way than presented by Welge. A typical B-L profile for drainage is shown in Fig. 3.

We will now derive, in an approximate approach, what the typical shape is of an I-Sw plot when a B-L shock front is present. First, it can be shown that the *average* saturation is constant when measured between the position of the shock front in the plug and point of injection. We denote that saturation by S_{w_bl}.

Therefore, in first approximation, the resistivity per unit length upstream of the front can be considered constant and determined by $S_{w\_bl}{}^{-n}$, assuming that the rock is characterised by some constant value of n. The resistivity per unit length downstream of the front is constant, since $S_w = S_{wi} = 1.0$ everywhere downstream of the front. The resistivity across the plug is now calculated as

$$R(t) = R_{upstr} + R_{downstr} \approx \frac{v_f t}{L} R_0 S_{w\_bl}^{-n} + \frac{(L - v_f t)}{L} R_0 \qquad \text{Eq. 6}$$

The average brine saturation in the plug is

$$S_{w\_avg}(t) = \frac{v_f t}{L} S_{w\_bl} + \frac{(L - v_f t)}{L} S_{wi} = \frac{v_f t}{L} S_{w\_bl} + \frac{(L - v_f t)}{L} \qquad \text{Eq. 7}$$

A typical log-log plot of $I(S_w) = R_t / R_0$ versus S_w is shown in Fig. 4, for $n = 2$ [10]. It should be noted that it is this data that would be produced by the CI experiment: total resistivity across the sample plotted against plug-averaged brine saturation. These CI data deviate significantly from the true $I(S_w)$ function. When applied to log calibration, one would take some value of I from the log, go into the measured graph and read the corresponding S_w. Clearly, deviations of 20 or more saturation units may occur (see Fig. 4).

Capillary pressure active

Going back to the formulation by Buckley and Leverett, it is clear that the presence of a capillary pressure will distort the shock front. In fact, it is the gradient of the capillary pressure that acts on the shape of the shock front, rather than the plateau level of the capillary pressure. Generally, the capillary pressure function can be described through a Leverett-J function

$$P_c(S_w) = s \cos q \sqrt{\frac{j}{K}} J(S_w) \qquad \text{Eq. 8}$$

The ratio of the capillary pressure gradient over the viscous pressure gradient will determine the distortion of the shock front. The viscous pressure gradient is proportional to $1/K$, so low-permeable samples are more prone to exhibit sharp shock fronts than high permeable ones.

To demonstrate the effect of capillary pressure, we have simulated [11] CI experiments, varying σ. Some results are presented in Fig. 5. Clearly, the capillary pressure gradient is controlling the shape of the plot.

It should be noted that at low P_c gradients, the flow rates at which capillary forces can overcome viscous forces may become too low to be practical or cost-effective in the laboratory: experiments could take several months per plug, assuming that such low flow rates can be handled reliably over prolonged period of time.

A second important effect that we observed is that there is a limit to lowering the injection rate. If the viscous forces are lowered more and more, the saturation distribution may become dominated by gravity forces. In that case, a distinct front (equivalent to the plateau of the capillary pressure function) will travel through the plug from top to bottom (CI experiments need to be conducted gravity stable, with injection of the less dense phase from the top). When plug characteristics bring us into this range, lowering the rate further does not change and improve the saturation profile anymore.

We will discuss in the next section how an SS flooding scenario will overcome the shortcomings of the standard CI method.

Displacement by Steady-State

In an SS experiment, brine and crude are injected simultaneously [7] at a specified f_w (Fig. 6). Injection is sustained until a steady state is achieved: saturations and pressure drop are then read-off to calculate relative permeability. Subsequently, f_w is changed to bring the plug to another saturation. In-between steady states, a transient period occurs during which a B-L profile moves through the sample. Modern SS apparatuses are equipped with in-situ saturation measurements employing gamma- or X-rays. Often a large throughput of liquids is required before a steady state is achieved and material balance becomes inaccurate for saturation measurement.

We have constructed an X-ray SS apparatus [12] that has multiple electrodes along the sample to measure resistivity at several parts of the plug. A moving X-ray source-detector system scans the saturation profile continuously. By reading resistivity across a portion of the sample and linking that data to the local saturation, we can measure the resistivity index without the problems caused by the shock front. Moreover, we can measure during the transient stage, provided that a significant shock front is not present within the sample between the electrodes. Also, if a significant end-effect would be present, we are still able to read resistivity reliably, again provided that no significantly curved saturation profile is present between the electrodes. In any case, the X-ray data will tell us what the shape is of the saturation profile.

If it is decided to pick up resistivity data only at steady state, in practice some 10 points will be generated. Although this method does not provide the same data density as delivered by the CI technique, 10 points in most cases will be more than adequate to characterise the resistivity index accurately.

Discussion

Currently, we employ our new X-ray SS apparatus routinely for combined relative permeability and resistivity index measurements, both in drainage and in imbibition mode. In those cases, where the gradient of the capillary pressure is large enough for a CI measurement, we still have the advantage that the resistivity index can be measured at no additional cost. We present results of such measurements on mixed-wet carbonate rock in another SCA 2000 contribution [6].

A general conclusion is that with this technology data can be generated not accessible by the CI method for some samples. On the other hand, resistivity index data obtained by the X-ray SS technique proved to be consistent with data from CI where expected.

As a standard procedure, we design SS experiments to optimally distribute steps in fractional flow to get both a proper spread of data points over the saturation range for resistivity and for relative permeabilities. An estimate for relative permeabilities and capillary pressure is then required as input in design calculations or simulations of the experiments. Subsequently, we compare actual data with predicted values on the fly and adjust the measurement protocol, also on the fly, accordingly.

It is important to note that the height of the shock front is never more than the jump in saturation "asked for" by the applied jump in f_w. This means that in SS mode, even if a shock front would travel between two electrodes during the resistivity measurement, the effect is much less than in a conventional CI experiment.

Measurement times with SS, also for low permeable samples, usually do not exceed two weeks. The SS method therefore is competitive with the CI technique in terms of equipment occupancy and turn-around time. On the other hand, CI equipment is much less complicated and therefore less expensive compared to SS. Below, we will derive analytical criteria to design CI experiments with acceptable artefacts due to B-L and gravity.

Condition for acceptable impact of saturation profile in CI experiments
A quantitative, albeit approximate, criterion can be derived as follows. Let us assume that a fairly flat saturation profile exists in the plug. For the resistivity measurements to be only minimally affected by the variation of saturation in the plug, we should require the spread ΔS_w to be small over the plug, around an average value of S_w. This then corresponds to a variation in capillary pressure across the plug of

$$\Delta P_c(S_w) = \Delta S_w \left(\frac{dP_c}{dS}\right)_{S=S_w} \qquad \text{Eq. 9}$$

Now, initially, S_w is large and therefore the water relative permeability is large too (starting at unity for drainage experiments). This will cause the pressure drop in the water phase to be much smaller than the pressure drop in the oil phase. Consequently, we find that ΔP_c will be close to the viscous pressure drop over the full length of the plug in the oil phase ΔP_o. Once the oil reaches the outflow end of the plug, we may calculate a matching oil injection rate by Darcy's equation:

$$q_o \approx \frac{k_{ro}(S_w)}{m_o} K \frac{\Delta P_o}{L} A \qquad \text{Eq. 10}$$

Obviously, this is only approximately correct. In the experiment only oil is injected and only water can be produced through the water-wet filter connected to the outflow end. So the flow rate of water and oil varies significantly through the plug.

Combining Eqs. 9 and 10, we have an approximate maximum rate for the oil where a reasonable saturation profile exists governed by the prevailing capillary pressure gradient and viscous pressure drop

$$q_{o,\max} = \frac{k_{ro}(S_w)}{m_o} K \frac{A}{L} \Delta S_w \left(\frac{dP_c}{dS}\right)_{S=S_w} \qquad \text{Eq. 11}$$

We note that $q_{o,\max}$ will be small for large S_w, since the oil relative permeability is then very low.

By combining Eq. 11 with Eq. 8, we get an expression that determines $q_{o,\max}$ as a function of all relevant parameters. $q_{o,\max}$ is proportional to $k_{ro}(S_w), \sqrt{jK}, s$ and $dJ(S_w)/dS$.

Since some severe assumptions were brought-in to derive this criterion, we have tested it extensively using numerical simulations. We used $\frac{1}{2}\Delta S_w = 0.05$ around an average value $S_w = .95$ as maximum allowable saturation range that we expected to give us a reasonable saturation profile and therefore a reasonable I-Sw plot. After choosing q_o, we kept the rate constant during the experiment. Excellent agreement was found: when q_o was set below $q_{o,\max}$ as calculated from Eq. 11, indeed, the I-Sw curve deviated from the ideal plot less than the chosen ΔS_w.

Given this result, there is scope to improve the CI measurement protocol further: during the injection, with decreasing water saturation the injection speed can be increased. When Eq. 11 is still honoured, curvature due to the B-L artefact is expected to be minimal. Significant cost reduction can be achieved, notably because $k_{ro}(S_w)$ and therefore $q_{o,\max}$ may increase by several orders of magnitude if S_w decreases. However, it remains important to verify such a protocol through simulations. At saturations close to S_{wc}, the pressure drop in the water phase will become important and Eq. 11 may not be valid.

Condition for acceptable impact of gravity in CI experiments

When gravity dominates viscous forces, a saturation height function will exist in the plug with $h(S_w) = P_c(S_w)/\Delta rg$. A saturation plateau will appear in the plug, if 1) P_c has a plateau and 2) $\Delta h(S_w)$, for the saturation range of the plateau, is much less than L, the length (height) of the plug. Therefore, no gravity artefacts on the I-Sw measurement by CI are expected if $\Delta h(S_w) > 10 * L$ or:

$$\Delta S \frac{dP_c}{dS} > 10 \Delta r g L \qquad \text{Eq. 12}$$

with ΔS the saturation range across the plateau and dP_c/dS the average capillary pressure gradient over the plateau.

Sensitivity to absolute permeability
Experimentally, we have seen the B-L artefact both in low and in high permeable plugs. This means that apparently the slope of the capillary pressure curve, which is here the important factor, does not correlate well with absolute permeability. Figs. 7 and 8 show respectively an example of a drainage capillary pressure curve measured on a highly permeable rock, and a typical resistivity plot for that rock type. The shape of the resistivity plot is quite similar to the plot in Figs. 4 or 5, although in this particular case we do not have conclusive evidence that the curvature is solely caused by the shock front.

In summary: we strongly recommend to check and design resistivity experiments for all samples using information of the capillary pressure curve and estimates of the relative permeabilities. For drainage (the most common experiment for log calibration), capillary pressure is easily obtained by a standard Hg-air measurement. Screening the design of a CI experiment is then straightforward, using Eqs. 11 and 12. These analytically derived criteria are only approximate. We recommend that simulations be used for verification when, for practical laboratory reasons, q_o would have to be set within one order of magnitude below $q_{o,\max}$ from Eq.11. Several simulator tools are available on market, including the free SCORES tool on the public Internet [13].

Moreover, once that a CI experiment is in progress and a curvature appears on the log-log plot, we recommend to vary the injection rate on the fly to check for sensitivity of this curvature against injection rate.

Conclusions

- Calculations and simulations have been used to prove the risk that exists in applying the CI technique for resistivity measurements under a weak capillary pressure gradient. Deviations of 20 saturation units or more are possible.
- In many cases the CI technique is adequate to determine the resistivity index.
- Easy to use criteria have been derived to assess risk of a B-L artefact or gravity effect that obscures I-Sw data by the CI method.
- Calculations or simulations are strongly recommended to assess likely failure of the CI technique due to an insufficient capillary gradient.
- Significant cost savings can be achieved by speed-optimising the CI measurement protocol for a given plug.
- In case a curved log-log resistivity plot develops, we recommend to test sensitivity of this curvature with flow rate.
- The SS technique provides a great alternative for the CI method if the capillary gradient is too small.
- If the SS technique is chosen, the resistivity index can be measured simultaneously with the relative permeabilities

Acknowledgement
We like to thank management of Shell Technology Exploration and Production in Rijswijk for permission to publish this paper.

Nomenclature

a	Humble constant	fraction
A	area	[m^2]
f	fractional flow	fraction
F	formation factor	fraction (ratio of sample conductivity over brine conductivity)
h	height	[m]
J	Leverett-J function	
k	relative permeability	fraction
K	absolute permeability	[m^2]
L	length	[m]
m	cementation index	
n	Archie exponent	
P	pressure	[Pa]
q	flowrate	[m^3/s]
R	resistivity	[Ω]
S	saturation	fraction
t	time	[s]
v	velocity	[m/s]

Greek

θ	contact angle	
μ	viscosity	[Pa.s]
σ	interfacial tension	[N/m]
φ	porosity	fraction

Subscripts

c	capillary, connate
downstr	downstream
f	front
o	oil
r	relative
t	total
w	water (brine)
0	initial
upstr	upstream

References

1 Zeelenberg, H.P.W., and Schipper, B.A., "Developments in I-Sw measurements", in *Advances in Core Evaluation II, Reservoir Appraisal*, Gordon and Breach Science Publishers, Philadelphia 1991, p. 257

2 Waxman, M.H., and Smits, L.J.M., "Electrical conductivities in oil-bearing shaly sands", SPE Journal, 8 (1968), p. 107

3 Hausenblas, M., "How wettability can affect rock resistivity - a case study", proc. 4th Intl. Symp. on Evaluation of Reservoir Wettability and its Effect on Oil Recovery, Montpellier, Sept. 1996.

4 Johnson, E.F., Bossler, D.P., and Naumann, V.O., "Calculation of relative permeability from displacement experiments", *Trans. AIME*, (1959) **216**, 370

5 de Waal, J.A., Smits, R.M.M., de Graaf, J.D., and Schipper, B.A., "Measurement and evaluation of resistivity index curves", SPWLA Thirtieth Annual Logging Symposium, June 11-14, 1989

6 van der Post, N., Masalmeh, S.K., Coenen, J.G.C., van der Gyp, K.H., and Maas, J.G., "Relative permeability, hysteresis and I-Sw measurements on a carbonate prospect", SCA 2000-7, paper to be presented at the Intl SCA Symp. Abu Dhabi, October 2000

7 Dake, L.P., *Reservoir Engineering*, Elsevier, Amsterdam, 1978

8 Welge, H.J., "A simplified method for computing oil recovery by gas or water drive", *Trans. AIME*, (1952) **195**, p. 91

9 Buckley, S.E., and Leverett, M.C., "Mechanism of fluid displacement in sands", *Trans. AIME*, (1942), **146**, p. 107

10 An accurate analysis can be conducted by either analytically integrating the upstream B-L profile, or by conducting detailed computer simulations of the experiment. The authors have verified that the approximate I-Sw curve presented in Fig. 4 is close to the results obtained by detailed simulations. Deviations are typically less than 5 saturation units.

11 Simulations were conducted using MoReS, the Shell Group reservoir simulator. MoReS was used as a fully implicit simulator, with 50-500 grid blocks in 1-D. First and last grid block were given a permeability by a factor 10 000 larger than of the grid blocks in the core plug. Other characteristics of the end blocks were that porosity was set to unity, relative permeabilities set to straight lines and Pc set to zero. In the core plug, Corey type relative permeabilities were used, with a typical water-wet signature: high exponent for water (6) and a lower exponent for oil (3). Generally, modelling was similar to as published in [13].

12 The apparatus is equipped with a Kevex PXS6 X-ray source. Measurement accuracy for saturation: 2 saturation units; for resistivity: 1%; for position along the core 0.01 mm. Electrodes are a combination of ring and point electrodes. For more details, please see: Coenen, J.G.C., and Koornneef, P., "State-of-the-art X-ray steady state apparatus for advanced core flow studies", SCA-9853, poster presented at the Intl. SCA Symp. The Hague, October 1998

13 Maas, J.G., and Schulte, A.M., “Computer simulation of Special Core Analysis (SCAL) flow experiments shared on the Internet”, SCA-9719 presented at the Intl. SCA Symp. Calgary, September 1997

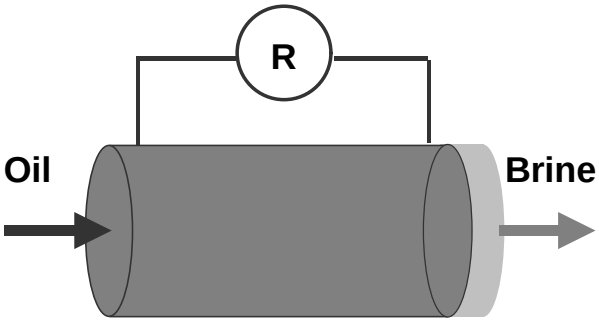

Fig. 1 Continuous injection measurement principle with water-wet filter at outflow end

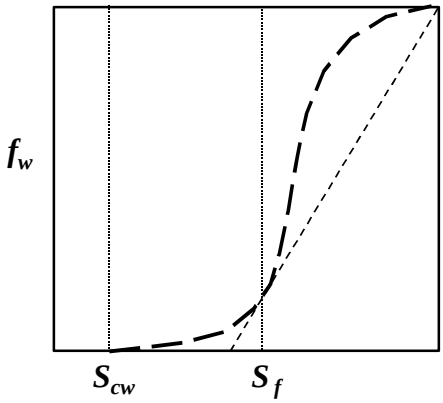

Fig. 2 Typical fractional flow curve for a drainage experiment, with Welge construction to find the shock front saturation S_f during drainage.

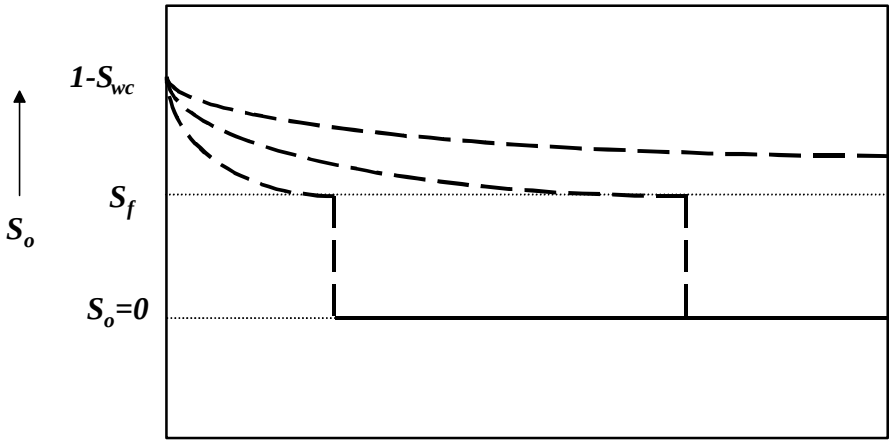

Fig. 3 Typical Buckley-Leverett saturation profile during drainage

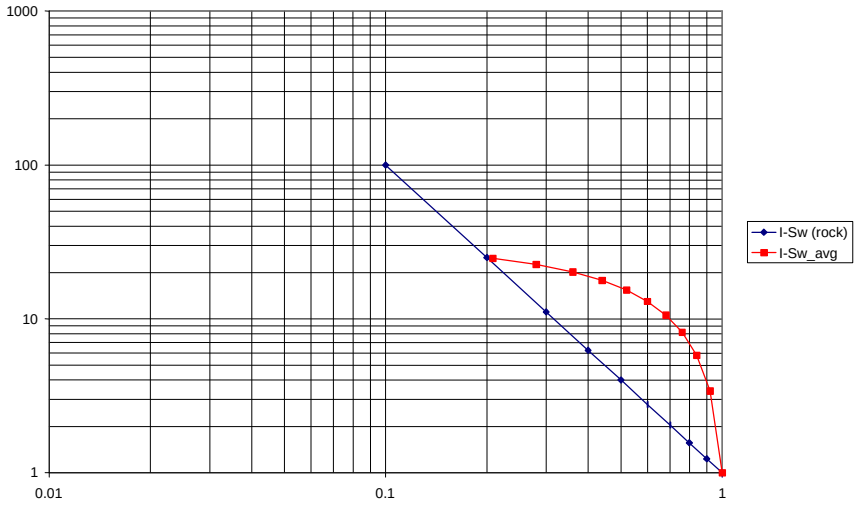

Fig. 4 Approximate resistivity index plot if a shock front arises in the CI equipment, compared to actual microscopic resistivity (n=2)

Cases 1 to 4 are modelled wtih decreasing capillary presure gradient

The microscopic resistivity index equals 2

It can be seen that the uneven saturation distribution causes the overall resistivity to be too high for low oil saturation (highwater saturation); the correct resitivity (for n=2) is eventually reached.

For clarity, the results have been displayed with increasing Ro values

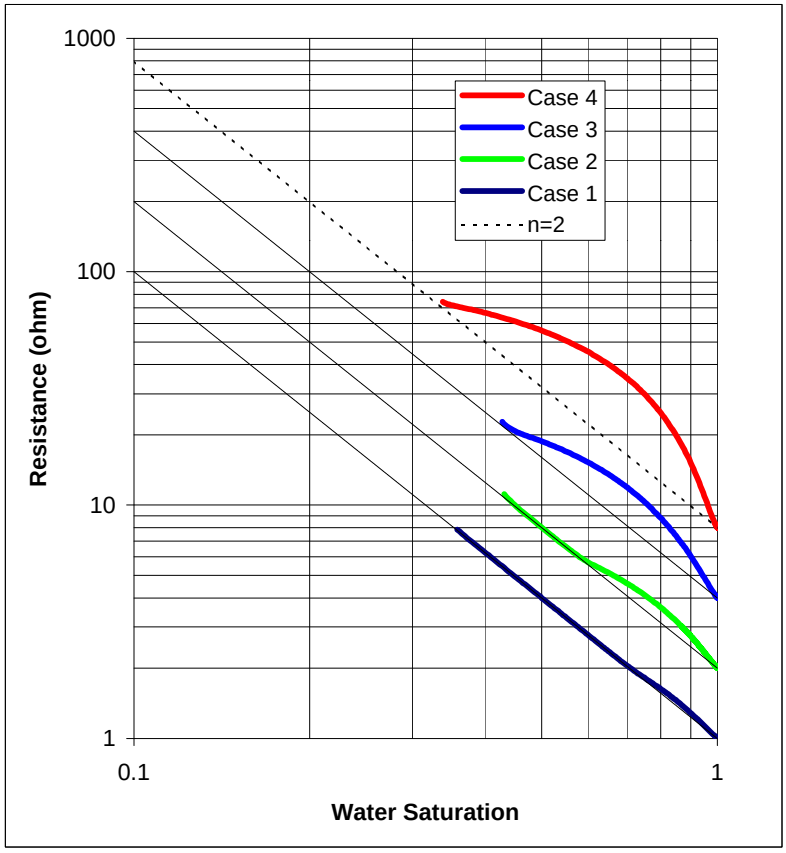

Fig. 5 Simulated resistivity index plots at several capillary pressure gradients

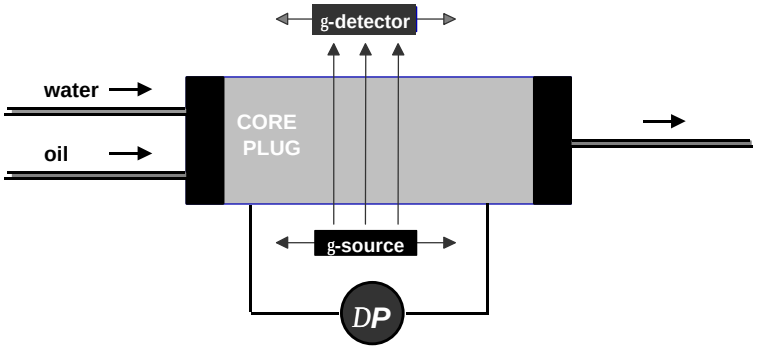

Fig. 6 Schematic of Steady-State experiment

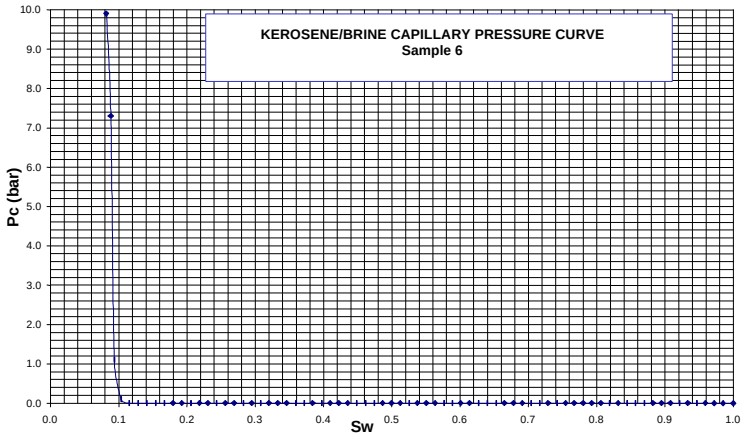

Fig. 7 Drainage capillary pressure curve measured with Hg-air, of same sample used in Fig. 8. Note that pressure measurement resolution here was 0.05 bar, and entry pressure (P_c at $S_w = 1.0$) and subsequent P_c plateau were found to be below resolution.

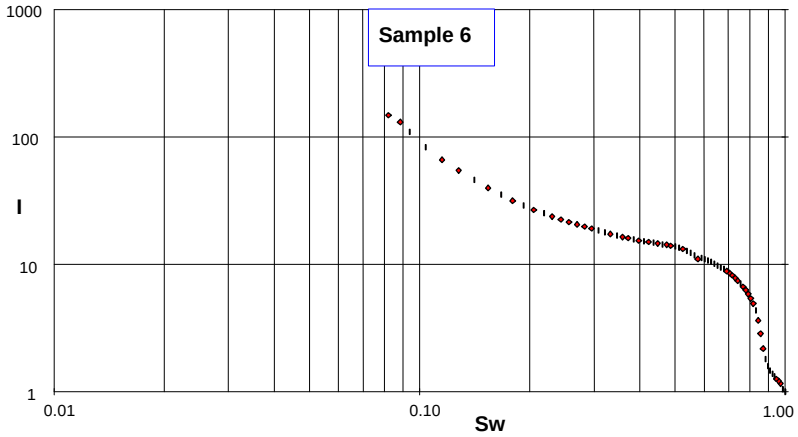

Fig. 8 Resistivity index measurement by Continuous Injection, high permeable sample (> 1D)